A simple approach to modelling the soil water budget in cool temperate mineral topsoils

Alison Brand[a], Allan Lilly[b] and Jo Smith[a]

alison.brand@abdn.ac.uk (corresponding author), allan.lilly@hutton.ac.uk, jo.smith@abdn.ac.uk

[a] Institute of Biological and Environmental Sciences, School of Biological Sciences, University of Aberdeen, 23 St Machar Drive, Aberdeen AB24 3UU, Scotland

[b] The James Hutton Institute, Craigiebuckler, Aberdeen AB15 8QH, Scotland

Abstract

A simple soil water budget model is introduced and evaluated against data collected at four sites at Gourdie, near Dundee, Scotland, during 2000, using both short-term (2000-only) and long-term (1961-2011) averaged climate data. The performance of the model is compared using five different pedotransfer function sets to derive parameters for cool temperate mineral soils.

Simulated soil water values were significantly correlated with measurements for all pedotransfer functions and climate-terms. The minimum total error achieved between simulations and measurements for the best performing pedotransfer function was 19%, suggesting that predictions are accurate to within 20% of the average measurement. A low bias was observed in the simulations when compared to measured values, suggesting only a small systematic overestimate (2.8% of average measurement). Some model assumptions may have been invalidated where extreme events such as storms or anomalous dry spells were not captured in the monthly time-step led to small model errors.

---

i. PTFs: Pedotransfer functions
ii. FC: Field capacity
iii. PWP: Permanent wilting point
iv. GWS: Gross water storage
v. PET: Potential evapotranspiration
vi. AET: Actual evapotranspiration
vii. SWRC: Soil water retention curve
viii. MVG: Mualem-van Genuchten
ix. PSMD: Potential soil moisture deficit
x. Sy-structured: ‘Sandy horizons with some structural development’
xi. Sy-unstructured: ‘Sandy horizons with no structural development’

Graphical Abstract

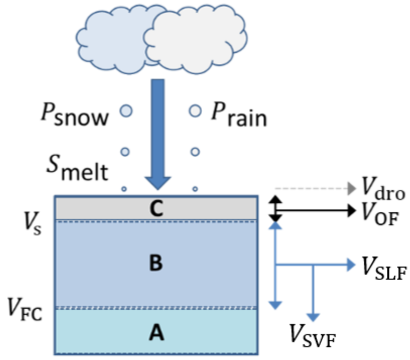

Precipitation input *is partitioned into rain,* P_{rain}*, snow,* P_{snow}*, and after a lag, snow meltwater,* S_{melt}*.* V_s *and* V_{FC} *represent the* ***soil water contents*** *at saturation and field capacity, respectively.* ***Drainage*** *consists of direct runoff (from impervious or sloping ground),* V_{dro}*, overland flow,* V_{OF}*, subsurface lateral flow,* V_{SLF}*, and subsurface vertical flow,* V_{SVF}*. The soil water level lies within: Box A,* $V_{OF} = V_{SLF} = V_{SVF} = 0$*; or Box B,* $V_{OF} = 0$*.*

Highlights

- Evaluates a tool to predict soil water budgets in the soil/ plant system
- Uses existing process-based models from scientific literature
- Driven by commonly available meteorological data and soil descriptions
- Five PTFs compared: Hollis et al. (2014) is best suited to Scottish soils
- Easily adaptable for different uses by other researchers

Keywords

Dynamic simulation modeling, soil water budget, pedotransfer functions, drainage, mineral soils.

1. Introduction

1.1. Problem definition

Policy makers often need to understand the effects of land use and climate change on soil water supply, plant growth, carbon storage, and nutrient loses. However, many soil water simulation models (e.g. SWATRE: Belmans et al., 1983; WAVE: Vanclooster et al., 1996; HYDRUS: Šimůnek et al., 2012) are too complex and require too many parameters to be used by non-specialists and to be easily applied at large scales.

1.2. Innovation

Here, a simple soil water model is introduced, which can be implemented using only the information available for the large-scale modelling required by policy makers. It has been written in Microsoft Excel so that it is transparent and easily accessible for different uses by other researchers. The model combines a new formulation of existing soil water models with a new initialisation method and integrates concepts originally derived for partitioning precipitation (Dingman, 2015) and drainage (McCabe and Markstrom, 2007; Dunn et al., 2004; Glugla, 1969, as cited in Bräunig, 2001; and Wolock and McCabe, 1999). A succinct description is presented here, which includes only the new components of the model.

The formulation has been used to test components of different combinations of soil water models. This allows those interested in functional soil water modelling to see the suitability of the components to different environments. This modular approach allows models to be constructed for different environments using sets of pedotransfer functions (PTFs[i]), which have been implemented and tested within the model. Pedotransfer functions are used to predict soil water properties from more readily available soil properties such as soil texture, where measured soil water properties are not available.

Most soil water simulation models use either continuous functions based on the relationship between soil water pressure head, water content and conductivity which are designed to solve the Richards equation (Hollis et al., 2014), or capacity-type functions based on water contents and/or air-filled porosities between specified soil water pressure heads (Hollis et al., 2014). Functions for modelling the continuous relationship between soil water pressure head- water content-conductivity in soils include HYPRES (Wösten et al., 1999) and HYDI (Tóth et al., 2015) for European soils. Capacity-type functions include: HYDI (Tóth et al., 2015) for European soils, and SEISMIC (Cranfield University, 2008) and UK-MIN (Hollis et al., 2014) for UK mineral soils.

The PTFs used here have been derived using data sets from different locations. Hence, it would be expected that PTFs would perform best in the environments for which equations were derived. Here we explicitly test the accuracy of the PTFs within a simple modelling framework using data derived for cool temperate mineral soils. We present an assessment of the uncertainty with which the model simulates net change in soil water in response to the effects of climate change on these mineral soils. The model assumes that similar processes can occur in all cool temperate mineral soils, but the extent of these processes is modified by the soil conditions. The soil water model is evaluated against data collected at four sites at Gourdie, near Dundee, Scotland during 2000, using both short-term (2000 only) and long-term (1961-2011) averaged climate data.

1.3. Aims

The water balance model described in this study is part of the "Soil Management Assessment Tool" (SoilMAT), which is being developed as a component of the soils work in the Scottish Government's Rural and Environment Science and Analytical Services Division (RESAS) 2016-21 Strategic Research Programme. SoilMAT aims to allow policy makers to use simple approaches to simulate the impact of changes in resource management on soils in Scotland. The aims of this study are to (1) describe the structure of the water balance model, (2) explain the methodology developed to initialise and run the model, and (3) present an evaluation of the different components of the soil water balance model.

2. Materials and Methods

2.1. Model structure

The model assumes water enters the soil from the top and leaching occurs as a 'piston flow' process (after Bradbury et al., 1993). Each layer down the profile is successively filled with water, before draining to the layer below. For simplicity, a single layer is used in SoilMAT to simulate water movement through the topsoil or to a depth of 30 cm, whichever is greater (Figure 1). This simplification is made as the monthly time-step is longer than would usually be required for water to move through the profile.

The soil water content at field capacity (FC[ii]), permanent wilting point (PWP[iii]) and saturation are estimated using a range of different PTFs as described in Section 2.1.1. The initial gross water storage (GWS[iv]) of a soil is crudely estimated by using FC as a proxy for the soil water storage at the beginning of a month. A model initialisation run provides monthly values for GWS storage at the start of the simulation (Section 2.1.2). The model is then run forward to calculate the fate of the net precipitation that enters the soil profile (Table 1: Eq 3 to Eq 8).

Table 1: *Simulation of soil water – water gain. †Input data. Sources of equations are given at the bottom of the table.*

Symbol	Variable	Value, data source or formula		Units	Reference
Gross soil water storage, V_{gstor} (initial)					
V_{gstor}	Gross soil water storage	$V_{\mathrm{FC}} + V_{\mathrm{wat}}$	*Eq 1*	mm	
V_{FC}	Horizon soil water content at field capacity	$\theta_{\mathrm{FC}} \left(\frac{z}{10}\right)$	*Eq 2*	mm	
θ_{FC}	Volumetric water content at field capacity	See Table 4 to Table 7		%	
z	Simulation depth	Soil measurements		cm	
Natural water input, V_{wat}, and partitioning of precipitation					
V_{wat}	Net water input	$(1 - 0.05)\, P_{\mathrm{rain}} + S_{\mathrm{melt}}$	*Eq 3*	mm month^{-1}	(1a, 1b)
P_{t}	†Monthly precipitation	Recorded weather data		mm	
P_{rain}	Rainfall	$F_{\mathrm{m}}\, P_{\mathrm{t}}$	*Eq 4*	mm month^{-1}	(2)
F_{m}	melt factor	$\begin{Bmatrix} 0, & T_{\mathrm{a}} \leq 0\ ^{\circ}\mathrm{C} \\ 0.167 T_{\mathrm{a}}, & 0\ ^{\circ}\mathrm{C} < T_{\mathrm{a}} < 6\ ^{\circ}\mathrm{C} \\ 1, & T_{\mathrm{a}} \geq 6\ ^{\circ}\mathrm{C} \end{Bmatrix}$	*Eq 5*		(2)
P_{snow}	Snowfall	$(1 - F_{\mathrm{m}})\, P_{\mathrm{t}}$	*Eq 6*	mm month^{-1}	(2)
S_{melt}	Meltwater from the monthly snowmelt	$F_{\mathrm{m}}\, (S_{\mathrm{pack,t-1}} + P_{\mathrm{snow}})$	*Eq 7*	mm month^{-1}	(2)
$S_{\mathrm{pack,t}}$	Snowpack water equivalent at the end of month t	$(1 - F_{\mathrm{m}})^2\, P_{\mathrm{m}} + (1 - F_{\mathrm{m}})\, S_{\mathrm{pack,t-1}}$	*Eq 8*	mm month^{-1}	(2)
$S_{\mathrm{pack,t\text{-}1}}$	Snowpack water equivalent at the end of previous month			mm month^{-1}	(2)

Sources: (1a) McCabe and Markstrom (2007); (1b) Wolock and McCabe (1999); (2) Dingman (2015).

The net precipitation (all of the meltwater and 95% of the rain) is assumed to infiltrate the soil (Table 1, Eq 3: McCabe and Markstrom, 2007; Wolock and McCabe, 1999). The remaining 5% of the rainfall is assumed to be lost by direct runoff from impervious surfaces or from infiltration excess overflow. Net precipitation (Table 1: partitioned into rain, snow or meltwater, after Dingman, 2015) enters the soil from the top, where it is added to existing soil water storage (Figure 1). Each layer down the profile is successively filled with water to FC. Any excess water is then drained to the layer below as subsurface vertical flow (Figure

1; Table 2), which will ultimately drain to groundwater (Figure 1; Table 2) (Dunn et al., 2004; Glugla, 1969, as cited in Bräunig, 2001[v]); or laterally as loss by subsurface lateral flow (Figure 1; Table 2) (Dunn et al., 2004).

Drainage from the soil is estimated by considering three different states in relation to field and saturation capacity (after Dunn et al., 2004):

- GWS < FC: no drainage from the soil column (Figure 1; Table 2)
- FC < GWS < saturation capacity (Figure 1; Table 2: Eq 9)
- GWS > saturation capacity (Figure 1; Table 2: Eq 10)

If the soil is saturated, excess water will drain from the soil surface as overland flow (Figure 1; Table 2: Eq 11) (Dunn et al., 2004). The model could potentially be adjusted to take account of input from direct run-on and surface lateral flow. It may be possible to account for direct run-on input by assuming that it is represented by the direct runoff output from the previous month and to revise the direct runoff output to monthly net change from direct runoff. Direct runoff is currently assumed to be 5% of rainfall, whereas net change in direct runoff would be less than this and hence negligible. More specific representation would not be appropriate in a non-spatially explicit model, such as this, with a monthly timestep.

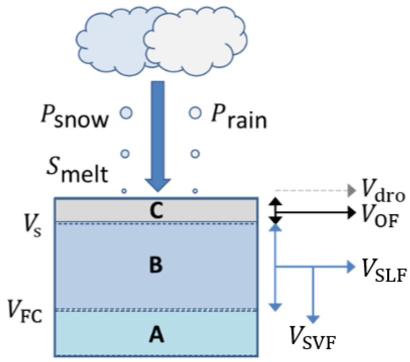

*Figure 1: **Precipitation input** is partitioned into rain, P_{rain}, snow, P_{snow}, and after a lag, snow meltwater, S_{melt}. V_s and V_{FC} represent the **soil water contents** at saturation and field capacity, respectively. **Drainage** consists of direct runoff (from impervious or sloping ground), V_{dro}, overland flow, V_{OF}, subsurface lateral flow, V_{SLF}, and subsurface vertical flow, V_{SVF}. The soil water level lies within: Box A, $V_{OF} = V_{SLF} = V_{SVF} = 0$; or Box B, $V_{OF} = 0$.*

***Table 2:** Simulation of soil water – water loss I. Note: Input data are shown in shaded cells.*

Symbol	Variable	Value, data source or formula		Units	Reference
Drainage, V_{drain}					
V_{drain}	Gross soil water storage < Field capacity (no drainage from the soil column)	0		mm month^{-1}	(1)
V_{drain}	Field capacity < gross soil water storage < saturation capacity	$V_{SLF} + V_{SVF}$	*Eq 9*	mm month^{-1}	(1)
V_{drain}	Gross soil water storage > saturation capacity	$V_{\mathrm{OF}} + V_{SLF} + V_{SVF}$	*Eq 10*	mm month^{-1}	(1)
V_{OF}	Loss to overland flow	$V_{gstor} - V_{\mathrm{s}}$	*Eq 11*	mm month^{-1}	(1)
V_{gstor}	Gross soil water storage	See Table 1	*Eq 1*	mm month^{-1}	
V_{FC}	Soil water content at field capacity	See Table 1	*Eq 2*	mm	
θ_{FC}	Volumetric water content at field capacity	See Table 4 to Table 7		%	
z	Simulation depth	Soil measurements		cm	
V_{wat}	Net water input	See Table 1	*Eq 3*	mm month^{-1}	(2a, 2b)
P_{rain}	Rainfall	See Table 1	*Eq 4*	mm month^{-1}	(1)
F_{m}	melt factor	See Table 1	*Eq 5*		(1)
P_{t}	Monthly precipitation	Recorded weather data		mm	
P_{snow}	Snowfall	See Table 1	*Eq 6*	mm month^{-1}	(1)
S_{melt}	Meltwater from the monthly snowmelt	See Table 1	*Eq 7*	mm month^{-1}	(1)
$S_{\mathrm{pack,t}}$	Snowpack water equivalent at the end of month t	See Table 1	*Eq 8*	mm month^{-1}	(1)
$S_{\mathrm{pack,t-1}}$	Snowpack water equivalent at the end of previous month			mm month^{-1}	(1)
V_{s}	Soil water content at saturation capacity	$\theta_{\mathrm{s}}\left(\frac{z}{10}\right)$	*Eq 12*	mm	

Symbol	Variable	Value, data source or formula		Units	Reference
θ_{s}	Volumetric water content at saturation capacity	See Table 4 to Table 7		%	
V_{SLF}	Average loss by subsurface lateral water loss through soil layer	$\left(\frac{1000}{7}\right)\left(\frac{(\min\{V_{gstor}, V_{s}\} - V_{FC})}{\Phi_{D}\, k_{L}}\right)$	Eq 13	mm month^{-1}	(1)
Φ_{D}	Drainable porosity or air capacity of a soil	$\Phi_{T} - \theta_{FC}$	Eq 14	%	(3)
Φ_{T}	Total porosity of a soil	$100\left(1 - \frac{\rho_{b}}{\rho_{p}}\right)$	Eq 15	%	(3)
ρ_{b}	Bulk density of the soil	Soil database		g cm^{-3}	
ρ_{p}	Particle density of the soil	$2.652 + 0.216\frac{P_{clay}}{100} - 2.237\frac{P_{OM}}{100}$	Eq 16	g cm^{-3}	(4)
P_{clay}	Clay content	Local measurements or soil database		%	
P_{OM}	Organic matter content	$1.724\, P_{C}$	Eq 17	%	
P_{C}	Carbon content	Local measurements or soil database		%	
k_{L}	Lateral flow calibration parameter	$\frac{1000\,(\min\{V_{gstor}, V_{s}\} - V_{FC})}{7\,\Phi_{D}\,(\min\{V_{gstor}, V_{s}\} - V_{FC} - V_{SVF})}$	Eq 18		(1)
V_{SVF}	Average loss by subsurface vertical water loss through soil layer	$\left(\frac{1000}{7}\right)\left(\frac{\Phi_{D}\,(\min\{V_{gstor}, V_{s}\} - V_{FC})}{k_{V}}\right)$	Eq 19	mm month^{-1}	(1)
k_{V}	Vertical flow calibration parameter	$\frac{10^{5}\, z^{2}\, \Phi_{D}}{7c\,(\min\{V_{gstor}, V_{s}\} - V_{FC})}$	Eq 20		(1)
c	Coefficient for gravitational water flow in water-saturated soil columns	$1692.6\,\exp\frac{10(\Phi_{D} - V_{FC})}{z}$	Eq 21	mm day^{-1}	(5)

Sources: (1) Dunn et al. (2004); (2a) McCabe and Markstrom (2007); (2b) Wolock and McCabe (1999); (3) Hollis et al. (2014); (4) Schjønning et al. (2017); (5) Glugla (1969, 1970; as cited in Bräunig, 2001).

Soil water is subject to evapotranspiration after any filling by precipitation or loss by drainage has occurred. Evapotranspiration takes place successively from layers down the profile as the upper layers empty. However, if the soil is bare, the model assumes that only the top 5 cm slice loses water and once emptied, no further loss occurs (i.e. upward movement of water from below is neglected). Potential evapotranspiration (PET[vi]) is calculated as described by Hamon (1963, as cited in Dingman, 2015; Table 3; Eq 22). This is multiplied by the proportion of the depth of simulations (30 cm or less depending on depth of topsoil) and the maximum rooting depth of the plant for the growing season (Table 3; Eq 27). A similar method was used for monthly actual evapotranspiration (AET[vii]) from the selected soil depth. Following the method of Dunn et al. (2004), AET rates were limited in relation to FC, to take account of very dry periods. The dynamic model run then follows a similar structure to the initialisation run (Section 2.1.3), with FC replaced by the initial GWS and AET at depth substituted for PET at depth.

The water available to a plant is calculated as the difference between the volumetric water content at FC and the water held in the soil at PWP; and is allowed to evaporate or be transpired by the plant down to the PWP.

***Table 3:** Simulation of soil water – water loss II. Note: Input data are shown in shaded cells.*

Symbol	Variable	Value, data source or formula		Units	Reference
Potential evapotranspiration, V_{PET}					
V_{PET}	Potential evapotranspiration (PET)	$29.8\, d_{\mathrm{month}}\, L \left(\frac{e^*(T_{\mathrm{a}})}{T_{\mathrm{a}}+273.2}\right)$	*Eq 22*	mm month^{-1}	(1)
d_{month}	Number of days in month				
T_a	Mean monthly temperature	Local measurements or weather database		°C	
L	Day length	$\left(\frac{24}{\pi}\right) \cos^{-1}(-\tan(\phi) \tan(\delta))$	*Eq 23*	h	(2)
$e^*(T_{\mathrm{a}})$	Saturation vapour pressure at the mean daily temperature	$0.61094 \exp\left(\frac{17.625 T_{\mathrm{a}}}{T_{\mathrm{a}}+243.04}\right)$	*Eq 24*	kPa	(3)
ϕ	Latitude	Local measurements		rad	
δ	Declination of the sun	$0.006918 - 0.399912 \cos(\theta_{\mathrm{d}}) + 0.070257 \sin(\theta_{\mathrm{d}}) - 0.006758 \cos(2\theta_{\mathrm{d}}) + 0.000907 \sin(2\theta_{\mathrm{d}}) - 0.002697 \cos(3\theta_{\mathrm{d}}) + 0.001480 \sin(3\theta_{\mathrm{d}})$	*Eq 25*	rad	(4)
θ_{d}	Date in Julian days expressed as an angle	$2\pi \left(\frac{d_j}{365}\right)$	*Eq 26*	rad	
d_j	Number of Julian days	0 on January 1st to 364 on December 31st			
$V_{\mathrm{PET,z}}$	PET from selected soil depth	$\min\left(V_{\mathrm{PET}}, V_{\mathrm{PET}}\left(\frac{z}{z_{\max}}\right)\right)$	*Eq 27*	mm	
V_{AET}	Actual evapotranspiration (AET)	$\begin{Bmatrix} V_{\mathrm{PET}}, & V_{\mathrm{wat}} \geq 0.7V_{\mathrm{FC}} \\ \frac{V_{\mathrm{PET}} V_{\mathrm{wat}}}{0.7V_{\mathrm{FC}}}, & otherwise \end{Bmatrix}$	*Eq 28*	mm month^{-1}	(5)
$V_{\mathrm{AET,z}}$	AET from selected soil depth	$V_{\mathrm{AET}}\left(\frac{z}{z_{\max}}\right)$	*Eq 29*	mm	
z	Simulation depth	Soil measurements		cm	
$z_{\max}$	Maximum rooting depth	Field observations for plants		cm	

Sources: (1) Hamon (1963) as cited in Dingman (2015); (2) after Kirk (2011) with revised conversion to radians; (3) August-Roche-Magnus formula (Lawrence, 2005); (4) Spencer (1971); (5) Dunn et al. (2004).

2.1.1. Pedotransfer functions

Knowledge of the soil water retention curve (SWRC[viii]) is essential for understanding and modelling soil hydraulic processes. However, direct determination of the SWRC is time consuming and costly, as soil hydraulic properties display high spatial and temporal variability. An alternative is the use of models, called pedotransfer functions (PTFs) (Bouma, 1989), which estimate the SWRC from easy-to-measure physical, morphological and chemical properties.

For soil water retention, one approach (using point PTFs and capacity-type regressions for soil texture classes), consists of estimating soil water contents at several soil water pressure heads (e.g. saturation, FC and PWP), using a separate predictive equation for each pressure head. Note that different authors define FC at different soil water pressure heads. Another approach (using parametric PTFs) involves estimating coefficients in equations that express the dependence of the water content on the soil water potential, e.g. using the Mualem-van Genuchten (MVG[ix]) continuous water retention model (Pachepsky and van Genuchten, 2011).

Mualem-van Genuchten continuous water retention model

The HYPRES (Wösten et al., 1999) PTFs were derived by firstly fitting the MVG water retention model to soil hydraulic data (van Genuchten (1980); Table 4: Eq 30). The EU-HYDI[1] (Tóth et al., 2015) used a similar approach to derive PTFs for United States Department of Agriculture (USDA) soil texture classes (Table 5: USDA, 1951).

These parameters were then related to soil properties, such as the proportion of sand, silt, clay and organic matter, and the soil dry bulk density through multiple regression equations (Table 6)

Table 4: *Simulation of soil water – Pedotransfer functions I. Note: Input data are shown in shaded cells.*

Symbol	Variable	Value, data source or formula		Units	Reference
1 Mualem-van Genuchten continuous water retention model					
$\theta(h)$	Water content of the soil at a given matric potential value	$\theta_r + \frac{\theta_s - \theta_r}{[1+(\alpha h)^n]^m}$	*Eq 30*	cm³ cm⁻³	(1)
h	Height of water column			cm	
1.1 HYPRES Mualem-van Genuchten parameters					
θ_r	Residual volumetric soil water content	$\begin{cases} 0.025, & P_{clay} < 18\% \text{ and } P_{sand} > 65\% \\ 0.01, & otherwise \end{cases}$	*Eq 31*	%	(2)
θ_s	Saturated volumetric soil water content	$0.7919 + 0.001691\,P_{clay} - 0.29619\,\rho_b - 0.000001491\,{P_{silt}}^2 + 0.0000821\,{P_{OM}}^2 + 0.02427/P_{clay} + 0.01113/P_{silt} + 0.01472\ln(P_{silt}) - 0.0000733\,P_{OM}\,P_{clay} - 0.000619\,\rho_b\,P_{clay} - 0.001183\,\rho_b\,P_{OM} - 0.0001664\,\mathrm{T}\,P_{silt}$	*Eq 32*	%	(2)
α	Curve fitting parameter	$\exp\,(-14.96\ + 0.03135\,P_{clay} + 0.0351\,P_{silt} + 0.646\,P_{OM} + 15.29\,\rho_b - 0.192\,\mathrm{T} - 4.671\,{\rho_b}^2 - 0.000781\,{P_{clay}}^2 - 0.00687\,{P_{OM}}^2 + 0.0449/P_{OM} + 0.0663\ln(P_{silt}) + 0.1482\ln(P_{OM}) - 0.04546\,\rho_b\,P_{silt} - 0.4852\,\rho_b\,P_{OM} + 0.00673\,\mathrm{T}\,P_{clay}$	*Eq 33*		(2)
m	Curve fitting parameter	$1-(1/n)$	*Eq 34*		(2)
n	Curve fitting parameter	$\exp\big(-25.23\ - 0.02195\,P_{clay} + 0.0074\,P_{silt} - 0.194\,P_{OM} + 45.5\,\rho_b - 7.24\,{\rho_b}^2 + 0.0003658\,{P_{clay}}^2 + 0.002885\,{P_{OM}}^2 - 12.81/\rho_b - 0.1524/P_{silt} - 0.01958/P_{OM} - 0.2876\ln(P_{silt}) - 0.0709\ln(P_{OM}) - 44.6\ln(\rho_b) - 0.02264\,\rho_b\,P_{clay} + (0.0896\,\rho_b\,P_{OM} + 0.00718\,\mathrm{T}\,P_{clay}\big) + 1$	*Eq 35*		(2)
T	Layer property	$\begin{cases} 1 & topsoil \\ 0 & otherwise \end{cases}$	*Eq 36*		(2)
ρ_b	Bulk density of the soil	Soil database		g cm⁻³	
P_{OM}	Organic matter content	See Table 2	*Eq 31*	%	
P_C	Carbon content	Local measurements or soil database		%	
P_{clay}	Clay content	Local measurements or soil database		%	

Symbol	Variable	Value, data source or formula		Units	Reference
P_{silt}	Silt content	Local measurements or soil database		%	
P_{sand}	Sand content	$100 - (P_{\mathrm{clay}} + P_{\mathrm{silt}})$	*Eq 37*	%	

Source: (1) Van Genuchten (1980); (2) Wösten et al. (1999)

.

***Table 5:** Simulation of soil water – Pedotransfer functions II. EU-HYDI[1] Mualem-van Genuchten parameters defined for USDA soil texture classes, where θ_s and θ_r are the saturated and residual volumetric soil water contents (%), respectively, $\theta(h)$ is the water content of the soil (cm^3 cm^{-3}) at a given matric potential value (h cm of water column), and α, m and n are curve fitting parameters as given in Table 4.*

USDA texture classes	θ_r (cm^3 cm^{-3})	θ_s (cm^3 cm^{-3})	α (cm^{-1})	n (-)	m (-)
sand	0.061	0.411	0.0258	1.8005	0.4446
loamy sand	0.052	0.475	0.0341	1.4846	0.3264
sandy loam	0	0.441	0.075	1.1904	0.1599
loam	0	0.491	0.0347	1.1931	0.1618
silt loam	0	0.424	0.0074	1.2545	0.2029
silt	0.009	0.465	0.0042	1.4853	0.3267
sandy clay loam	0	0.409	0.07	1.1335	0.1178
clay loam	0	0.465	0.1284	1.116	0.104
silty clay loam	0	0.463	0.0107	1.1892	0.1591
sandy clay	0.192	0.523	0.0351	1.4455	0.3082
silty clay	0	0.455	0.0309	1.111	0.0999
clay	0	0.499	0.0234	1.12	0.1072
organic	0.111	0.697	0.0069	1.4688	0.3192

Source: Tóth et al. (2015)

Point PTFs

The point PTFs where soil water contents were predicted separately at several points on the soil water content/pressure head continuum (e.g. saturation, FC and PWP that were used in SoilMAT were obtained from Tóth et al. (2015: EU-HYDI[2], Table 6: Section 1.1), Cranfield University (2008: SEISMIC for mineral soils, Table 6: Section 1.2) and Hollis et al. (2014: UK mineral soils, Table 6: Section 1.3 and Table 7).

***Table 6:** Simulation of soil water – Pedotransfer functions III. Note: Input data are shown in shaded cells.*

Symbol	Variable	Value, data source or formula		Units	Reference
1. Point PTFs for mineral soils					
V_*	Water content at defined pressure head*	$\theta_* \left(\frac{z}{10}\right)$	*Eq 38*	mm	
z	Simulation depth	Soil measurements		cm	
1.1 EU-HYDI[2] volumetric water content at defined pressure heads					
θ_s	Saturation (at 0 kPa)	$68.19 - 6.48\left(\frac{1}{1+P_C}\right) - 11.90({\rho_b}^2) - 2.668\,(T) + 0.1489(P_{clay}) + 0.08031(P_{silt}) + 2.321\left(\frac{1}{1+P_C}\right)({\rho_b}^2) + 1.908({\rho_b}^2)(T) - 0.1109(P_{clay})(T) - 0.002315(P_{silt})(P_{clay}) - 0.01197(P_{silt})({\rho_b}^2) - 0.01068(P_{clay})({\rho_b}^2)$	*Eq 39*	%	(1)
θ_{FC}	Field capacity (at -33 kPa)	$24.49 - 18.87\left(\frac{1}{1+P_C}\right) + 0.4527(P_{clay}) + 0.1535(P_{silt}) + 0.1442(P_{silt})\left(\frac{1}{1+P_C}\right) - 0.00511(P_{silt})(P_{clay}) + 0.08676(P_{clay})\left(\frac{1}{1+P_C}\right)$	*Eq 40*	%	(1)
θ_{PWP}	Permanent wilting point (at -1,500 kPa)	$9.878 + 0.2127(P_{clay}) - 0.08366(P_{silt}) - 7.67\left(\frac{1}{1+P_C}\right) + 0.003853(P_{silt})(P_{clay}) + 0.233(P_{clay})\left(\frac{1}{1+P_C}\right) + 0.09498(P_{silt})\left(\frac{1}{1+P_C}\right)$	*Eq 41*	%	(1)
T	Layer property	See Table 4	*Eq 36*		(1)
ρ_b	Bulk density of the soil	Soil database		g cm^{-3}	
P_C	Carbon content	Local measurements or soil database		%	
P_{clay}	Clay content	Local measurements or soil database		%	
P_{silt}	Silt content	Local measurements or soil database		%	
1.2 SEISMIC volumetric water content at defined pressure heads for Scottish soils					
θ_s	Saturation (at 0 kPa)	$102.593 - 37.4785\,(\rho_b)$	*Eq 42*	%	(2)
θ_{FC}	Field capacity (at -5 kPa)	$64.82 + 1.414(P_C) - 14.504(\rho_b) - 0.185(P_{silt})$	*Eq 43*	%	(2)

Symbol	Variable	Value, data source or formula		Units	Reference
θ_{INT}	Intermediate decomposition inhibition limit (at 200 kPa)	$20.235 + 1.497(P_C) + 0.289(P_{clay})$	Eq 44	%	(2)
θ_{PWP}	Permanent wilting point (at -1,500 kPa)	$17.266 + 1.007(P_C)$	Eq 45	%	(2)
ρ_b	Bulk density of the soil	Soil database		g cm^{-3}	
P_C	Carbon content	Local measurements or soil database		%	
P_{silt}	Silt content	Local measurements or soil database		%	
1.3 UK-MIN volumetric water content at defined pressure heads for UK mineral soils with potential soil moisture deficit (PSMD^x) of less than about 130 mm (defined for British Standard Texture Classifications)					
θ_s	Saturation (at 0 kPa)	$\Phi_T - \Phi_D F_{\theta_0}$	Eq 46	%	(3)
Φ_T	Total porosity of a soil	See Table 2	Eq 21	%	(3)
Φ_D	Drainable porosity or air capacity of a soil	See Table 2	Eq 20	%	(3)
F_{θ_0}	Fraction of drainable porosity	$-0.55 + 0.519 \log_{10}(\Phi_D) + 0.338 \rho_s - 0.0042 P_{sand}$	Eq 47		(3)
ρ_p	Particle density of the soil	See Table 2	Eq 30	g cm^{-3}	(4)
ρ_s	Structural density of the soil	$\rho_b + (0.009 P_{clay})$	Eq 48	g cm^{-3}	(3)
θ_{FC}	Field capacity (at -5 kPa)	See Table 4 to Table 7		%	(3)
θ_{INT}	Intermediate decomposition inhibition limit (at 200 kPa)	See Table 4 to Table 7		%	(3)
θ_{PWP}	Permanent wilting point (at -1,500 kPa)	See Table 4 to Table 7		%	(3)
ρ_b	Bulk density of the soil	Soil database		g cm^{-3}	
P_C	Carbon content	Local measurements or soil database		%	
P_{OM}	Organic matter content	See Table 2	Eq 31	%	
P_{clay}	Clay content	Local measurements or soil database		%	
P_{silt}	Silt content	Local measurements or soil database		%	

Symbol	Variable	Value, data source or formula		Units	Reference
P_{sand}	Sand content	See Table 4	*Eq 37*	%	

Sources: (1) Tóth et al. (2015); (2) Cranfield University (2008); (3) Hollis et al. (2014); (4) Schjønning et al. (2017).

Hollis et al. (2014) proposed a set of PTFs to determine water retention properties of UK mineral (UK-MIN) soils (Table 7) using British Standard Texture Classification (British Standards Institution, 1981).

This set of PTFs is based on a structural stratification of soil textures as given by Hollis et al. (2014):

- very fine sandy horizons (rare in Scotland and not discussed further here);
- other sandy texture horizons show very weak or no structural development and thus water retention is dependent principally on particle-size distribution and organic matter content:
  - ‘Sandy horizons with some structural development’ (Sy-structured[xi]);
  - ‘Sandy horizons with no structural development’ (Sy-unstructured[xii]);
- other regularly cultivated Ap horizons (Ap):
  - Topsoil horizons (excluding those with sandy textures) that are subject to regular cultivation undergo cycles of structural disruption and rearrangement, which are likely to have a significant impact on their soil water-retention properties; and
- all other horizons (excluding regularly cultivated Ap horizons) subdivided according to their packing or structural density:
  - ‘Horizons with low packing density’ (< 1.40 g cm^{-3}): usually very or extremely porous;
  - ‘Horizons with medium packing density’ (1.40 – 1.75 g cm^{-3}): usually moderately or slightly porous;
  - ‘Horizons with high packing density (> 1.75 g cm^{-3}) or with a stagnic colour pattern’: slowly permeable.

Sandy soils are further classified as:

- Sy-unstructured:
  - Soils derived from fluvial deposits with texture class (loamy sand (LS) or sand (S))
- Sy-structured:
  - All other loamy sand (LS) or sand (S) textures

Table 7: Simulation of soil water – Pedotransfer functions IV. UK-MIN volumetric water content at defined pressure heads for UK mineral soils with potential soil moisture deficit (PSMD) of less than about 130 mm (defined for British Standard Texture Classification) where θ_s, θ_{FC}, θ_{INT} and θ_{PWP} are the volumetric water contents (% volume) at saturation, field capacity, the intermediate decomposition inhibition limit and permanent wilting point, respectively.

Structural group	Pressure head (kPa)	PTF equations
Structure ordered by sandy texture or soil layers with no structural development		
Sandy-structured	-5	$\theta_{FC} = 7.74 + 11.195 \log_{10}(P_C) + 5.019 \left(P_{clay}\right)^{0.5}$
	-200	$\theta_{INT} = 2.04 + 9.036 \log_{10}(P_C) + 4.019 \left(P_{clay}\right)^{0.5}$
	-1,500	$\theta_{PWP} = 1.37 + 5.33 \log_{10}(P_C) + 2.83 \left(P_{clay}\right)^{0.5}$
Sandy-unstructured	-5	$\theta_{FC} = 7.13 + 1.013\, P_{silt}$
	-200 [a]	$\theta_{INT} = 1.16 + 1.392 \left(P_{clay}\right)^{0.5} + 0.481\, P_{silt}$
	-1,500	$\theta_{PWP} = 0.95 + 1.681 \log_{10}(P_C) + 1.784 \left(P_{clay}\right)^{0.5} + 0.243\, P_{silt}$
Ap-regularly cultivated	-5	$\theta_{FC} = 36.56 + 15.62 \log_{10}(P_C) - 8.09\, \rho_b + 1.209 \left(P_{clay}\right)^{0.5} + 0.053\, P_{silt}$
	-200	$\theta_{INT} = 10.84 + 14.418 \log_{10}(P_C) + 2.261 \left(P_{clay}\right)^{0.5} + 0.049\, P_{silt}$
	-1500 [b]	$\theta_{PWP} = 6.31 + 12.643 \log_{10}(P_C) + 2.131 \left(P_{clay}\right)^{0.5}$
Structure ordered by packing density		
Low (ρ_s< 1.4 g cm^{-3})	-5	$\theta_{FC} = 65.55 + 5.504 \log_{10}(P_C) - 23.838\, \rho_b + 0.522 \left(P_{clay}\right)^{0.5}$
	-200	$\theta_{INT} = 25.45 + 2.155 \log_{10}(P_C) - 8.322\, \rho_b + 2.18 \left(P_{clay}\right)^{0.5} + 0.066\, P_{silt}$
	-1,500	$\theta_{PWP} = 23.58 - 10.261\, \rho_b + 1.959 \left(P_{clay}\right)^{0.5}$
Medium (1.4 g cm^{-3} ≤ ρ_s ≤ 1.75 g cm^{-3})	-5 [c]	$\theta_{FC} = 70.44 - 29.502\, \rho_b + 1.572 \left(P_{clay}\right)^{0.5}$
	-200	$\theta_{INT} = 43.82 - 21.619\, \rho_b + 2.758 \left(P_{clay}\right)^{0.5}$
	-1,500	$\theta_{PWP} = 22.47 - 12.95\, \rho_b + 3.35\left(P_{clay}\right)^{0.5}$
High (ρ_s > 1.75 g cm^{-3})	-5	$\theta_{FC} = 96.75 - 39.544\, \rho_b + 0.045\, P_{silt}$
	-200	$\theta_{INT} = 80.45 - 36.533\, \rho_b + 0.665 \left(P_{clay}\right)^{0.5} + 0.055\, P_{silt}$
	-1,500	$\theta_{PWP} = 51.96 - 25.558\, \rho_b + 1.593 \left(P_{clay}\right)^{0.5} + 0.07\, P_{silt}$
	0	$\theta_s = \Phi_T - \Phi_D\, F_{\theta_0}$

Source: Hollis et al. (2014)

- Soils derived from fluvial deposits with texture class (sandy loam (SL) or sandy peat)

Note that the set of PTFs from the Hollis et al. (2014) supplementary information document are used for Scottish soils. These were independent of potential soil moisture deficit (PSMD) as a soil moisture deficit of greater than 130 mm is relatively rare in a Scottish context. In addition, fine sands were omitted from the PTF formulae, as soils with fine sand textures are not a common component of Scottish soils. This equates to a difference of approximately 8% in FC values.

The Hollis PTFs require soil bulk density as an input; however, these data were lacking for the soils used in the study. Instead, a database of around 800 measurements of soil bulk density along with soil texture and organic carbon concentrations held as part of the Scottish Soils Database at the James Hutton Institute were used to develop a set of regression equations to predict the soil bulk density (Gakgas pers comm, 2019). Drainable porosity or air capacity (Eq 14) and total porosity (Eq 15) of a soil were then subsequently determined using the relationships given in Hollis et al. (2014). Particle density was calculated as defined by Schjønning et al. (2017) (Eq 16). Renger's equation and classifications for packing or structural density were used (as cited in Hollis et al., 2014) (Eq 48).

All PTF volumetric water content values were adjusted for topsoil depth (to a maximum assumed depth of 30 cm), to give the total amount of water held in the topsoil at specific states: saturation, FC and PWP (Eq 38).

2.1.2. Initialisation of soil water storage

The following section is explained in greater detail as it describes the novel parts of the model.

The crude initial estimate of GWS (Section 2.1) is refined to give the initialised net soil water storage as described below (Table 8; Eq 49). First the GWS is distributed over the year using a soil water distribution factor (Table 8; Eq 50), the water lost to drainage is removed (Table 2) and the PET adjusted for plant and layer depth (Table 3).

Soil water distribution factor

The soil water distribution factor (Table 8; Eq 50) represents the monthly increment removed from soil storage due to loss processes (after Dingman, 2015). Soil water storage for two consecutive months changes according to the following relationship (Dingman, 2015):

$$V_{\mathrm{m-1}} - V_{\mathrm{m}} = V_{\mathrm{m-1}}\left[1 - \exp\left(-\frac{V_{\mathrm{PET}} - V_{\mathrm{wat}}}{V_{\mathrm{stor,max}}}\right)\right]$$

Rearranging this equation gives:

$$\frac{V_{\mathrm{m}}}{V_{\mathrm{m-1}}} = \exp\left(-\frac{V_{\mathrm{PET}} - V_{\mathrm{wat}}}{V_{\mathrm{FC}}}\right)$$

The relationship given in the above equation is used as the soil water distribution factor, f_{m}, to partition the crude initial estimate of GWS across the different months in the year (Table 8; Eq 50):

Table 8: *Initialisation of soil water storage. Note: Input data are shown in shaded cells.*

Symbol	Variable	Value, data source or formula		Units	Reference
Gross soil water storage, V_{gstor}					
V_{stor}	Monthly net soil water storage	$f_m V_{gstor} - V_{drain} - V_{PET,z}$	*Eq 49*	mm month^{-1}	(1)
V_{gstor}	Gross soil water storage	See Table 1 and Table 9	*Eq 1*	mm month^{-1}	
V_{drain}	Drainage from the soil column	See Table 2		mm month^{-1}	
$V_{PET,z}$	PET from selected soil depth	See Table 3	*Eq 27*	mm	
f_m	Soil water distribution factor	$\exp\left(-\frac{V_{PET} - V_{wat}}{V_{FC}}\right)$	*Eq 50*		(1)
V_{PET}	Monthly PET	See Table 3	*Eq 22*	mm	(2)
V_{wat}	Net water input	See Table 1	*Eq 3*	mm month^{-1}	(3a, 3b)
V_{FC}	Soil water content at field capacity	See Table 1	*Eq 51*	mm	
V_m	Soil water storage for month m				(1)
V_{m-1}	Soil water storage for month $(m-1)$				(1)
$V_{stor,max}$	*Water content at FC	V_{FC}	*Eq 52*	mm	(1)
f_{sat}	Saturation adjustment factor	$\frac{V_{stor}}{V_s}$	*Eq 53*		
V_s	Soil water content at saturation capacity	See Table 2	*Eq 12*	mm	
f_{sim}	Monthly simulated smoothed adjustment factor				
V_{istor}	Initial monthly adjusted net soil water storage	$\min\left\{\max\left\{\frac{V_{stor}}{f_{sim}}, V_{PWP}\right\}, 0\right\}$	*Eq 54*	mm month^{-1}	
V_{PWP}	Soil water content at permanent wilting point	See Table 6		mm	

Sources: (1) after Dingman (2015); (2) Hamon (1963) as cited in Dingman (2015); (3a) McCabe and Markstrom (2007); (3b) Wolock and McCabe (1999)

*Note: This definition digresses from Dingman (2015), where $V_{stor,max} = \theta_{FC}\, z_{max}$, with θ_{FC} being the volumetric water content at FC (%) and z_{max} is the maximum rooting depth (cm).

$$f_{\mathrm{m}} = \exp\left(-\frac{V_{\mathrm{PET}} - V_{\mathrm{wat}}}{V_{\mathrm{FC}}}\right)$$

Using the soil water distribution factor leads to a realistic pattern of soil water storage over the year. However, this approach often results in predicted values that are outside of the expected range for GWS, i.e. upper values may be greater than the saturated water content of the soil. Hence, the actual soil water storage is limited to being within set bounds for GWS, calculated as described in the next section.

Soil water storage boundaries

The upper bound of the initialised net soil water storage is capped by assuming that soil water storage is at saturation in Scotland in January. This is achieved using a saturation adjustment factor, f_{sat}, calculated for each month (Table 8; Eq 53):

$$f_{\mathrm{sat}} = \frac{V_{\mathrm{stor}}}{V_{\mathrm{s}}}.$$

In order to generate a pattern for f_{sat} that can be used in the forward simulations, a 6th order polynomial of the form:

$$ax^6 + bx^5 + cx^4 + dx^3 + ex^2 + fx + g,$$

is fitted to the annual trend of f_{sat} values (Figure 2) and the coefficients, a to g, are determined. The equation for the polynomial is used to determine simulated monthly smoothed adjustment factors, f_{sim} (Figure 2).

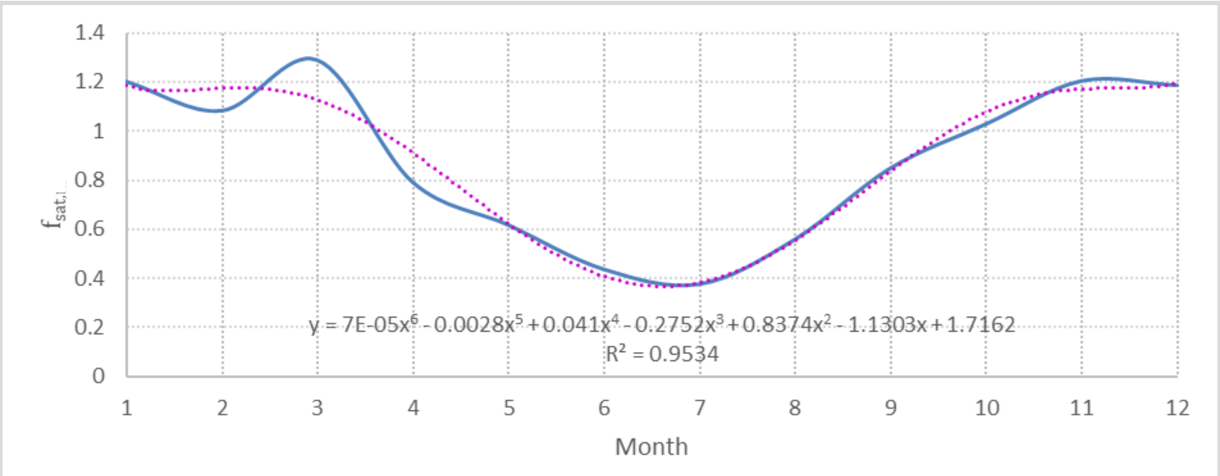

Figure 2: Example of the annual trend of the monthly saturation adjustment factors, f_{sat}, (solid), showing the monthly associated fitted 6th order polynomial (dotted) which gives the simulated smoothed adjustment factors, f_{sim}

The lower bound of the initialised net soil water storage is limited to the PWP, to give the final adjusted net soil water storage, V_{fstor} (Table 8; Eq 54):

$$V_{\mathrm{istor}} = \min\left\{\max\left\{\frac{V_{\mathrm{stor}}}{f_{\mathrm{sim}}}, V_{\mathrm{PWP}}\right\}, 0\right\}.$$

2.1.3. Determination of soil water storage

The dynamic model run follows the same model structure as the initialisation run. However, two of the inputs are changed:

- FC is replaced by the initial GWS in the calculation of GWS; and
- PET from selected soil depth is replaced by AET from selected soil depth

Table 9: *Determination of soil water storage. Note: Input data are shown in shaded cells.*

Symbol	Variable	Value, data source or formula		Units	Reference
Gross soil water storage, V_{gstor}					
V_{stor}	Monthly net soil water storage	$f_{\mathrm{m}}\, V_{\mathrm{gstor}} - V_{\mathrm{drain}} - V_{\mathrm{AET,z}}$	*Eq 55*	mm month^{-1}	(1)
V_{gstor}	Gross soil water storage	$V_{\mathrm{istor}} + V_{\mathrm{wat}}$	*Eq 56*	mm month^{-1}	
V_{drain}	Drainage from the soil column	See Table 2		mm month^{-1}	
$V_{\mathrm{AET,z}}$	AET from selected soil depth	See Table 3	*Eq 29*	mm	
f_{m}	Soil water distribution factor	See Table 8	*Eq 50*		

Sources: (1) after Dingman (2015).

2.2. Model Evaluation

2.2.1. Calculating uncertainty

Good model performance is indicated statistically by simulations and measurements that are both coincident (indicating a close fit) and associated (indicating the trends in measurements are replicated) (Smith and Smith 2007). As the Gourdie data set is not replicated, the degree of coincidence was determined by calculating the total error as the root mean squared error, RMSE (%), and the bias in the error as the mean difference, M (mm) (Addiscott and Whitmore, 1987). The association between simulated and measured values was calculated as the correlation coefficient, and the significance of the correlation was determined using a t-test (Smith and Smith, 2007). The t-test assumptions of normally distributed and independent data were ensured by assessing the simulations of change in soil moisture instead of total soil water, as individual measurements of total soil moisture might have been related to the previous value and so been non-independent. Sources of model error were also examined using graphical plots.

2.3. Soil water data for model evaluation

The Gourdie site is located to the north west of Dundee, Scotland adjacent to Royal Dundee Liff Hospital (GB OS national grid NO344328) at an altitude of between 50 and 95 m above Ordnance Datum. The site has a southerly aspect and slopes range from level (0°) to 5°. Three of the soils (Airntully, Buchanyhill and Carpow Series) were classed as freely drained Brown earths (Cambisols, IUSS Working Group WRB, 2015) and therefore had no inhibition to downward percolation of water. The fourth soil (Carey Series) was classed as an imperfectly drained Brown earth (also a Cambisol) with some evidence of seasonal waterlogging due to its low-lying position in the landscape. All four soils were sampled prior to the installation of experiments to monitor changes in soil moisture content over time. The particle size classes and percentage carbon needed as model input data were determined in the laboratory on air-dried, sieved (to < 2 mm) soil. The proportions of sand, silt and clay were determined by the hydrometer method and classified into the British Standard particle size classes with clay < 2 µm, silt 2-60 µm and sand 60-2000 µm (British Standards Institution, 1981). The carbon concentration (%) was measured using an elemental analyser on ball-milled, air-dried soil (Table 10). During the monitoring period, all sites were planted with winter barley, which was left to stubble following harvest.

The water content of the topsoils of the four different soil types were monitored at weekly intervals between 18/08/1999 and 13/12/2000 using a handheld ML1 Theta probe ™ (Delta T Devices). The sample areas were 10 x 10 m square and measurements were made at 2 m intervals giving up to 25 measurements per plot per week using the standard calibrations for mineral soils (Gaskin and Miller, 1996). Monthly topsoil water content sample means were determined for each plot. Data were not available for all sampling points for all weeks during the 16-month period.

Table 10: Soil series and composition of the field sites at Gourdie, Dundee

Soil Series	National Grid Reference	Soil Composition			
		Clay (%)	**Silt (%)**	**Sand (%)**	**Carbon (%)**
Buchanyhill	NO 346 325	22	41	37	2.52
Airntully	NO 351 324	14	39	47	3.01
Carpow	NO 352 323	16	31	53	2.00
Carey	NO 351 325	7.5	25.5	67	3.23

2.4. Input requirements for the water storage model

In this study, the following essential user supplied data inputs were input to run the soil water storage model:

- Location and soil composition data as detailed in Table 10.
- Soil layer depth: 30 cm
- Climate data were sourced automatically from long term 50-year average UKCP09 5 km x 5 km gridded rainfall and temperature data (Met Office, 2011) for the given locations on a monthly time step.
- Plant type during the monitoring period was winter barley, left to stubble following harvest.
- Growing season: September to August the following year.

3. Results and Discussion

3.1. Simulations of the stored water

The simulated and measured values of change in soil moisture were highly associated, unbiased and displayed coincidence at an acceptable RMSE of 10.0-11.2%, depending on the PTF used.

The simulated soil water content was plotted against the measured values of soil water content in the topsoil of the four sites sampled at Gourdie in 2000, for each of five PTFs that were used to predict the soil water parameters that were used to parameterise the simulation model, and using both short-term averaged climate data from 2000 (Figure 3) and long-term climate data averaged from 1961-2011 (Figure 4). The 1:1 lines which represent perfect agreement between the simulations and the measurements, are shown on the plots. The spread of points around the 1:1 line indicates the errors in the simulations of soil water compared to the measurements.

The correlation coefficient between the simulated and measured values for all of the PTFs used is highly statistically significant ($p < 0.0001$), with r varying from 0.63 to 0.76 using the short-term climate data (Table 11), and from 0.76 to 0.85 using the long-term climate data (Table 12). Hence there is a strong degree of association between the simulated and measured values, particularly for the long-term climate data. The UK-MIN PTF model (Hollis et al., 2014) gives the highest r^2 value (0.73).

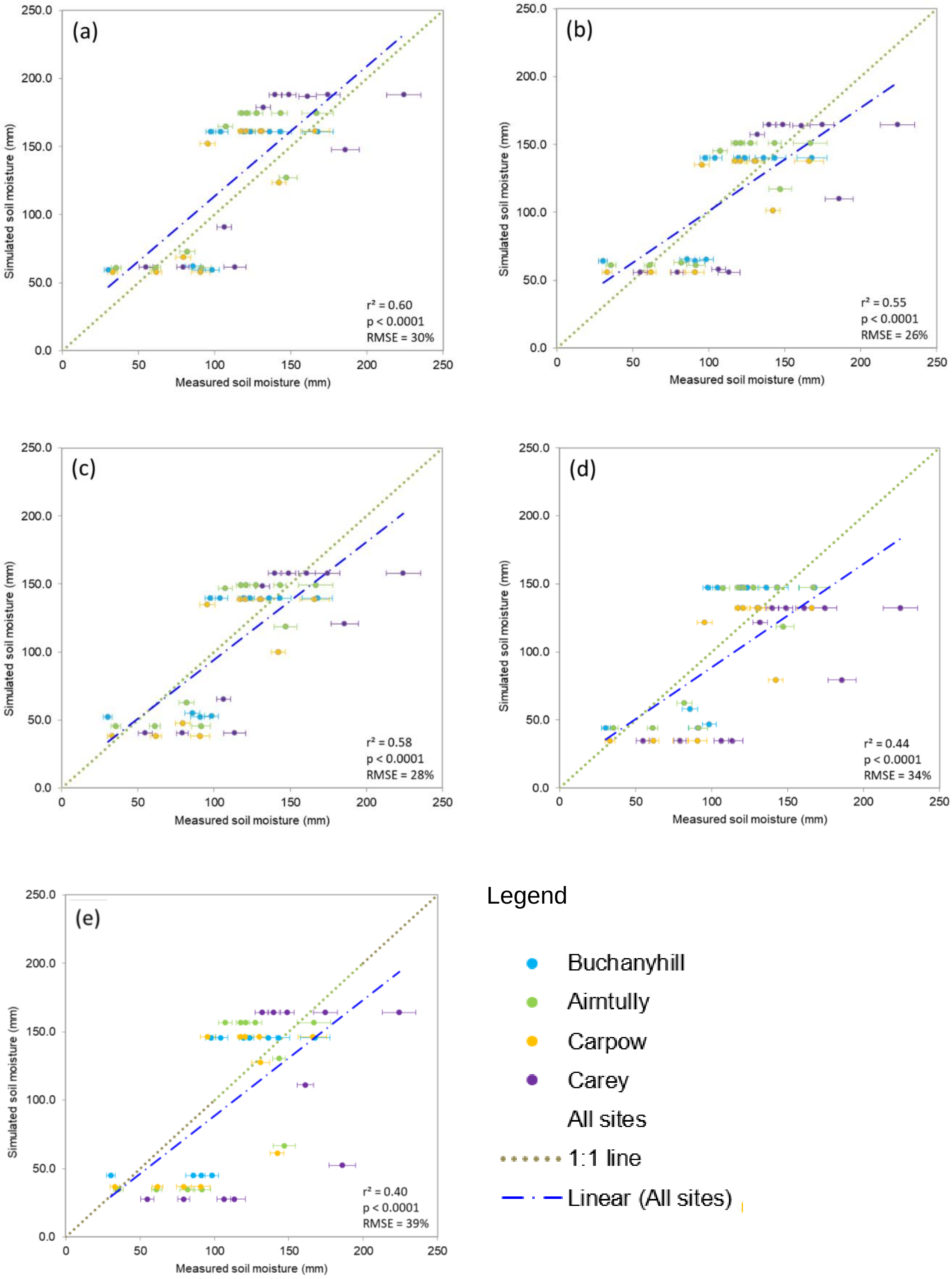

Figure 3: Comparison of simulated against measured values of soil water in the topsoil of four sites sampled at Gourdie in 2000, using short-term averaged climate data from 2000. Values have been calculated using five different PTFs: (a) SEISMIC (Cranfield University, 2008); (b) UK mineral soil (Hollis et al., 2014); (c) HYPRES (Wösten et al., 1999); (d) EU-HYDI[1] (Tóth et al., 2015); and (e) EU-HYDI[2](Tóth et al., 2015).

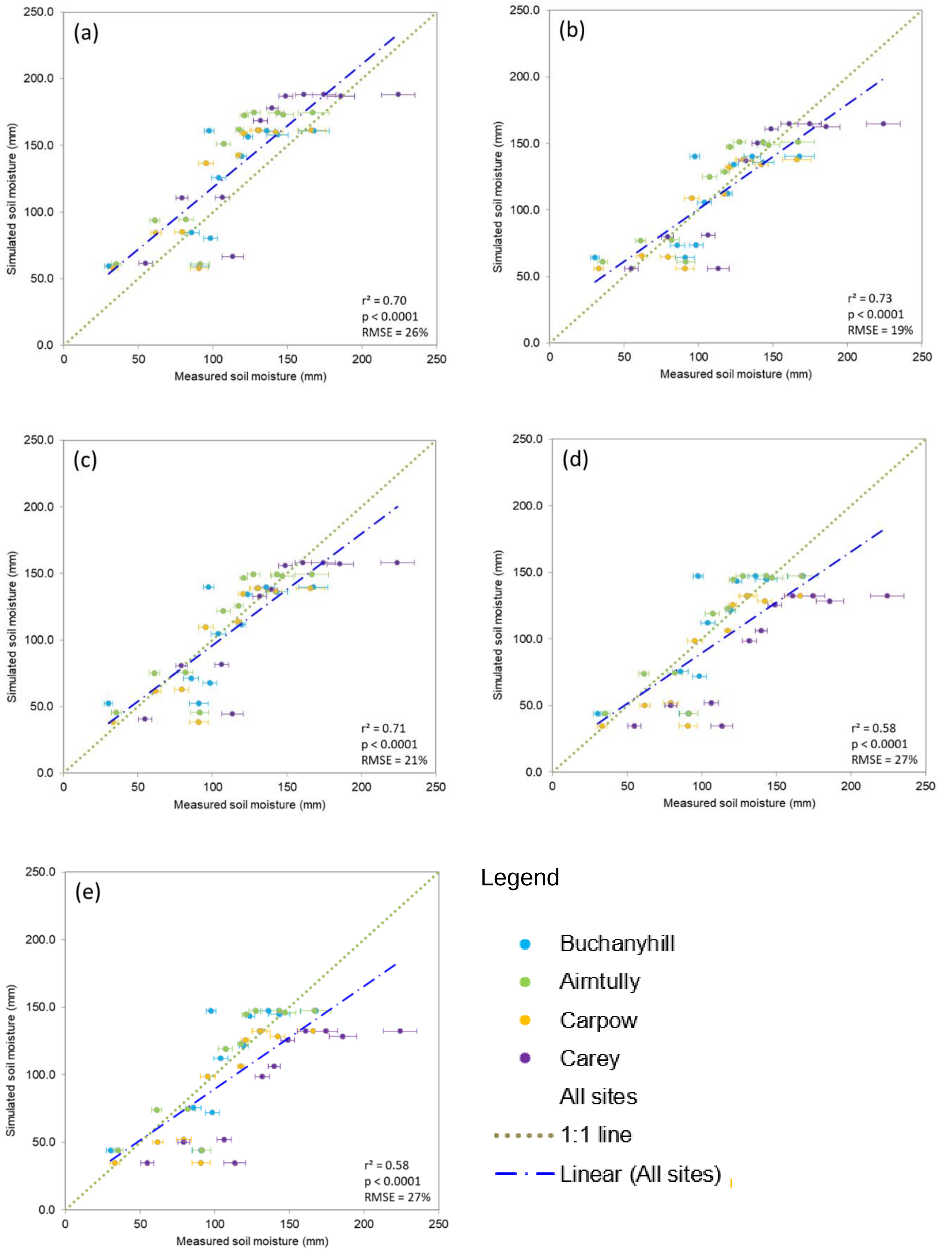

Figure 4: Comparison of simulated against measured values of soil water in the topsoil of four sites sampled at Gourdie in 2000, using long-term climate data averaged from 1961-2011. Values have been calculated using five different PTFs: (a) SEISMIC (Cranfield University, 2008); (b) UK mineral soil (Hollis et al., 2014); (c) HYPRES (Wösten et al., 1999); (d) EU-HYDI[1] (Tóth et al., 2015); and (e) EU-HYDI[2] (Tóth et al., 2015).

The mean differences (*M*) were small and not significantly different from zero for the UK-MIN PTF model for both climate data sets (Table 11 and Table 12) and for the HYPRES PTF model (Wösten et al., 1999) for the long-term climate data (Table 12). Statistics show small systematic deviations of simulation from measurement for the UK-MIN PTF and HYPRES PTF models, using the long-term data set, as the simulations were generally within about 20% of the measurements (Table 12). The bias in the simulations, as indicated by the mean difference (Addiscott and Whitmore, 1987) is low at 2.8% for UK-MIN (Table 12), suggesting only a small systematic overestimate (2.8%) when this PTF model is used.

Table 11: Evaluation of the degree of association and coincidence between simulated values using the Gourdie data (n = 44 for each pedotransfer function (PTF)), and using the short-term climate data averaged from 2000. RMSE: root mean squared error; r: correlation coefficient; M: mean difference; and E: relative error.

---------------PTF--------------		**--------Association---------**		**-------------------Coincidence-------------------**			
Type	**Model name**	**r**	**Degree of association**	**RMSE (%)**	**M**	**E****	**Bias**
Mualem-van Genuchten continuous functions	EU-HYDI[1]	0.67***	strong	34	15.06 ± 5.24	12.04	yes
	HYPRES	0.76***	strong	28	7.9 ± 5.24	5.82	yes
Point PTFs	EU-HYDI[2]	0.63***	strong	39	13.74 ± 5.24	12.13	yes
	SEISMIC	0.77***	strong	30	-12.86 ± 5.24	14.08	yes
	UK-MIN	0.74***	strong	26	2.68* ± 5.24	2.21	no

Note: *** represents $p < 0.0001$, which is considered to be highly significant

** 95% confidence interval of relative error, $E_{95} = 4.54$

* represents $p > 0.05$, which is considered to be insignificant

Sources: EU-HYDI[1] (Tóth et al., 2015); and HYPRES (Wösten et al., 1999); EU-HYDI[2] (Tóth et al., 2015); SEISMIC (Cranfield University, 2008); UK MIN (Hollis et al., 2014).

This comparison of PTFs in relation to Scottish soils suggests that Scottish soils have slightly different soil water retention properties to those in the rest of the UK and Europe (Cranfield University, 2008). Scottish soils tend to be more carbon-rich and are subject to different climatic conditions which may be driving the differences seen in observed *vs* predicted soil hydrological properties. Although the correlations between simulations and measurements are highly significant for all PTFs, both the EU-HYDI[1] and EU-HYDI[2] PTFs (Tóth et al., 2015) gave rise to the highest total errors (lowest coincidence reflected in high RMSE values) (Table 11 and Table 12) and were amongst the poorest performers. However, the EU-HYDI PTFs (Tóth et al., 2015) were developed for continental-scale applications in Europe. Tóth et al. (2015) noted that the organic carbon content of a soil is important in describing soil water properties as mineral soils with greater organic carbon content tend to have better soil structure, and thus increased water-holding properties, and organic matter itself also has good water-absorption properties. In general, the SEISMIC PTFs consistently overestimated soil water (Figure 3 and Figure 4). Cranfield University (2008) noted that their predictions for PTFs using Scottish data were particularly poor for topsoil (adjusted $r^2 < 0.5$), which may explain why the SEISMIC PTFs also performed poorly.

Table 12: Evaluation of the degree of association and coincidence between simulated values using the Gourdie data (n = 44 for each pedotransfer function (PTF)), and using the long-term climate data averaged from 1961-2011. RMSE: root mean squared error; r: correlation coefficient; M: mean difference; and E: relative error.

--------------PTF-------------		--------Association---------		-------------------Coincidence-------------------			
Type	**Model name**	**r**	**Degree of association**	**RMSE (%)**	**M**	**E****	**Bias**
Mualem-van Genuchten continuous functions	EU-HYDI[1]	0.76***	strong	27	14.13 ± 5.24	10.46	yes
	HYPRES	0.84***	strong	21	6.6* ± 5.24	3.56	no
Point PTFs	EU-HYDI[2]	0.83***	strong	26	10.62 ± 5.24	10.37	yes
	SEISMIC	0.85***	strong	26	-17.14 ± 5.24	19.16	yes
	UK-MIN	0.85***	strong	19	2.38* ± 5.24	2.76	no

Note: *** represents $p < 0.0001$, which is considered to be highly significant

** 95% confidence interval of relative error, $E_{95} = 4.54$

* represents $p > 0.05$, which is considered to be insignificant

Sources: EU-HYDI[1] (Tóth et al., 2015); and HYPRES (Wösten et al., 1999); EU-HYDI[2] (Tóth et al., 2015); SEISMIC (Cranfield University, 2008); UK MIN (Hollis et al., 2014).

The UK-MIN PTFs (Hollis et al., 2014) were the top performers with the lowest total error (19%) and no significant evidence of bias (Table 12), as they were developed with solely UK data. Hollis et al. (2014) used a structurally-based stratification of UK mineral soils, including a consideration of porosity. This agrees with Hollis et al.'s (2014) suggestion that the PTFs that they derived are most appropriate when applied across the whole of the UK. They clarified this by stating that more 'accurate' local predictions may potentially be made by deriving PTFs from relevant local data.

The best performing continuous MVG PTFs were those of Wösten et al. (HYPRES: 1999), who determined soil hydraulic properties based on soil texture. These PTFs were derived using the HYPRES database which holds data mainly from Western European Countries (Wösten et al., 1999). They also discussed other shortcomings of the HYPRES-based PTFs which included unpublished accuracy figures and lack of consideration of chemical properties, which may improve hydraulic predictions in certain cases (Wösten et al., 1999). Wösten et al. (1998) showed that the HYPRES PTFs are based on data with a bias towards Fluvisols, Cambisols and Gleysols (IUSS Working Group WRB, 2015). These soils have average topsoil organic matter concentrations of 3.44% and median 2.19%) which is below the average for Scottish soils perhaps limiting the usefulness of these PTFs for many Scottish soils. More accurate local predictions could likely be made using PTFs derived from relevant locally derived data.

Climate data is inherently variable and some of the discrepancies between simulation and measurement of soil water were most likely to be caused by extreme events, such as storms in the growing season, which tended to invalidate some of the model assumptions. An example of the fit of the water supply model using the UK-MIN PTFs and the long-term climate data to the Gourdie data is presented in Figure 5. Note that the soil water model is bounded by PWP and saturation and thus will not reflect soil water values outside this range. July 2000 was unusually dry, whilst waterlogging was observed in the ruts of compacted soil left by tractor tyres during a very wet December, at both the Buchanyhill and Carey sites.

4. Conclusions

A simple, but dynamic, soil water model driven by only simple input data has been described and estimates of the soil water throughout the year evaluated. This model will be easily adaptable for different uses by other researchers as it is highly transparent, on account of being written in Excel, highly modular and is documented in detail. Different modules could easily be incorporated by replacing existing modules, allowing the functionality of the rest the model to be used with any new additions. This soil water module is used within a wider model, SoilMAT, which has been developed for use by policy makers under funding from the Scottish Government. The SoilMAT model allows process-based dynamic simulation modelling of soil water to be used directly by policy makers to estimate impacts on soil organic matter turnover, nitrate leaching, greenhouse gas emissions, erosion risk and crop production. Note that this is a point-based model, with no representation of position in the landscape. It could be used to provide leaching loads, but if a spatial representation of movement through the landscape is required, more spatial data describing position in the catena would be needed.

It is often not easy to find appropriate data to test the model on, as it is rare to find both soil water data and all physical soil properties, especially clay content, reported for the same data set.

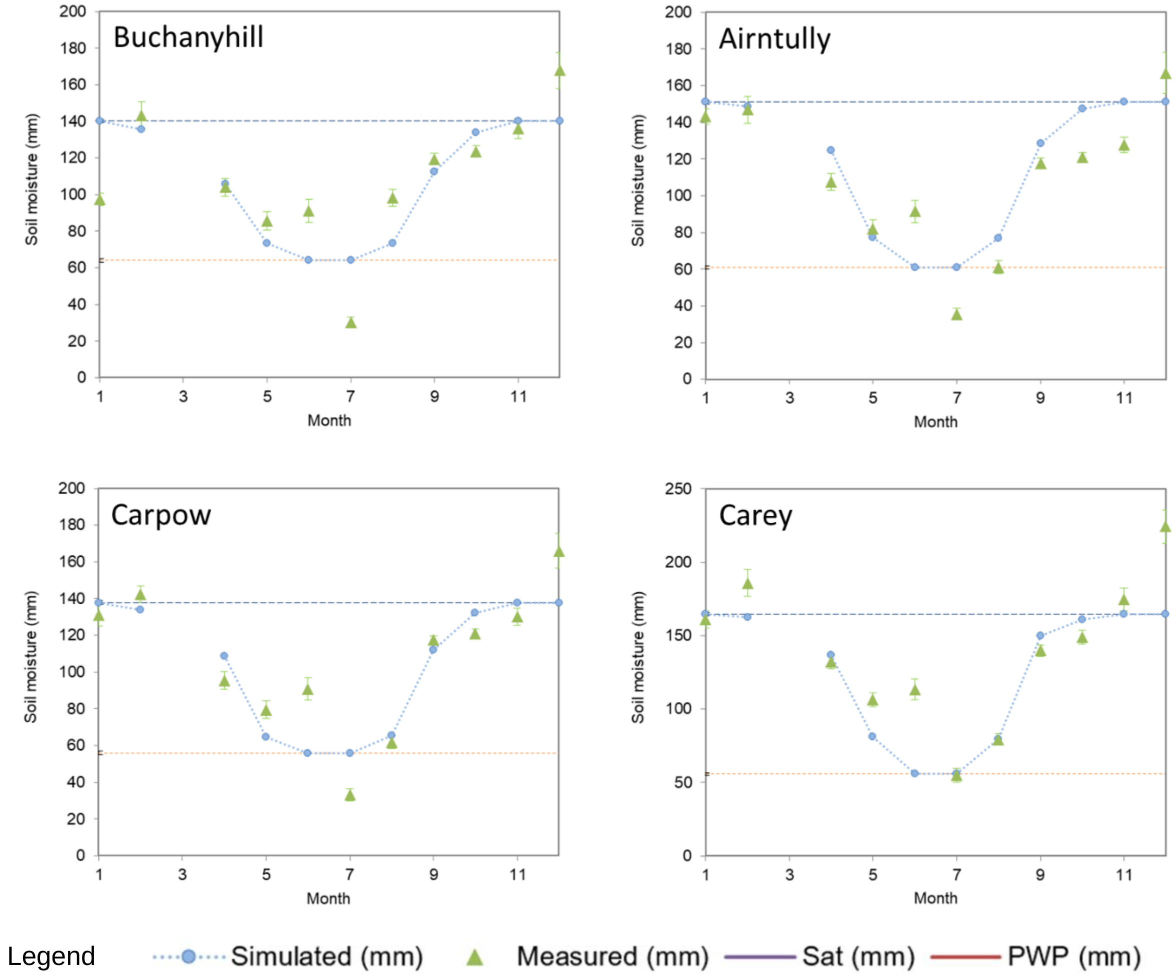

Figure 5: Comparison of simulated against measured values of soil water in the topsoil of four sites sampled at Gourdie during 2000, using long-term climate data averaged from 1961-2011. Values have been calculated using the UK mineral soil PTFs (Hollis et al., 2014). Note that no measurements were recorded for March 2000, as the ground was frozen.

Five PTFs were tested for use with cool temperate mineral topsoils. The predicted values of soil water generally agree to within 20% of the measurements for two of the PTF models, the UK-MIN and the continuous HYPRES models, using long-term climate data. Of these two models, the more 'local', point PTF UK-MIN model, which is based on UK-only data, performed better than the more 'generic', continuous HYPRES model. This was to be expected, given the location-specific nature of PTFs, although it is useful to note that the generic HYPRES PTFs provide a good alternative. Therefore, for Scottish conditions the UK-MIN model is the most appropriate model to use.

However, it should be noted that PTFs including PSMD as a predictor variable (e.g. UK-MIN) are likely to be less reliable if applied to areas with climatic characteristics outside those covered by the UK (Hollis et al., 2014).

Small model errors may have resulted from extreme events such as storms or anomalous dry spells in the growing season, not being captured in the monthly time-step. This may have invalidated some of the model assumptions.

5. Acknowledgements

Funding: This work was supported by the Rural and Environmental Science and Analytical Services (RESAS) Division of the Scottish Government [grant number RG13483]. RESAS played no further part in the study.

Author contributions: A.B., A.L. and J.S. designed the research; A.B. and A.L. performed the research; A.B. analysed the data; and A.B., A.L. and J.S. wrote the paper.

Declarations of interest: None

6. References

Addiscott, T.M., Whitmore, A.P., 1987. Computer simulation of changes in soil mineral nitrogen and crop nitrogen during autumn, winter and spring. *The Journal of Agricultural Science* 109, 141–157. https://doi.org/10.1017/S0021859600081089

Belmans, C., Wesseling, J.G., Feddes, R.A., 1983. Simulation model of the water balance of a cropped soil: SWATRE. *Journal of Hydrology* 63, 271–286. https://doi.org/10.1016/0022-1694(83)90045-8

Bouma J. (1989) Using Soil Survey Data for Quantitative Land Evaluation. In: Stewart B.A. (eds) Advances in Soil Science. *Advances in Soil Science*, vol 9. Springer, New York, NY. https://doi.org/10.1111/ejss.12509

Bradbury, N.J., Whitmore, A.P., Hart, P.B.S., Jenkinson, D.S., 1993. Modelling the fate of nitrogen in crop and soil in the years following application of 15N-labelled fertilizer to winter wheat. *The Journal of Agricultural Science* 121, 363. https://doi.org/10.1017/S0021859600085567

Bräunig, A. 2001. Entwicklung forstlich rekultivierter sowie renaturierter böden und simulation ihres wasserhaushaltes in der Mitteldeutschen Braunkohlen-Bergbaufolgelandschaft. Dissertation doctor rerum naturalium. Freiberger

Forchungshefte C489 Geoökologie. Technischen Universität Bergakademie Freiberg. 181pp. plus appendices.

British Standards Institution, 1981. Code of Practice for Site Investigations. BS5930:1981 Second Edition. British Standards Institution, London.

Cranfield University, 2008. *Major upgrade of SEISMIC to extend to the whole of Great Britain*. Final Report, Defra No. PS2225A, 19pp. http://randd.defra.gov.uk/Default.aspx?Module=More&Location=None&ProjectID=14489

Dingman, S.L., 2015. *Physical Hydrology*: Third Edition. Waveland Press.

Dunn, S.M., Lilly, A., DeGroote, J., Vinten, A.J.A., 2004. Nitrogen risk assessment model for Scotland: II. Hydrological transport and model testing. *Hydrology and Earth System Sciences Discussions* 8, 205–219. https://doi.org/10.5194/hess-8-191-2004

Gaskin, G.J and Miller, J.J.D., 1996. Measurement of soil water content using a simplified impedance measuring technique. *J. agric. Eng Res*. 63, 153-160.

Hamon, W.R., 1963. Computation of direct runoff amounts from storm rainfall. *Intl. Assoc. Scientific Hydrol. Publ*. 63, 52–62.

Hollis, J.M., Lilly, A., Higgins, A., Jones, R.J.A., Keay, C.A., Bellamy, P., 2014. Predicting the water retention characteristics of UK mineral soils: Soil water retention characteristics of UK mineral soils. *European Journal of Soil Science* 66, 239–252. https://doi.org/10.1111/ejss.12186

IUSS Working Group WRB. 2015. World Reference Base for Soil Resources 2014, update 2015 International soil classification system for naming soils and creating legends for soil maps. World Soil Resources Reports No. 106. FAO, Rome

Kirk, J.T.O., 2011. *Light and Photosynthesis in Aquatic Ecosystems*. Third edition. Cambridge University Press

Lawrence, M.G., 2005. The Relationship between Relative Humidity and the Dewpoint Temperature in Moist Air: A Simple Conversion and Applications. *Bulletin of the American Meteorological Society* 86, 225–233. https://doi.org/10.1175/BAMS-86-2-225

McCabe, G.J., Markstrom, S.L., 2007. A Monthly Water-Balance Model Driven by a Graphical User Interface (USGS Numbered Series No. 2007–1088), Open-File Report. Geological Survey (U.S.)

Met Office, 2011. *Long term (1960-2011) 5 km x 5 km gridded rainfall and temperature data*. http://www.metoffice.gov.uk/climatechange/science/monitoring/ukcp09/available/monthly.html (Accessed 18 October 2016)

Pachepsky, Y.A., van Genuchten, M.Th., 2011. Pedotransfer Functions, in: Gliński, J., Horabik, J., Lipiec, J. (Eds.), Encyclopedia of Agrophysics. Springer Netherlands, Dordrecht, pp. 556–561. https://doi.org/10.1007/978-90-481-3585-1_109

Schjønning, P., McBride, R.A., Keller, T., Obour, P.B., 2017. Predicting soil particle density from clay and soil organic matter contents. *Geoderma* 286, 83–87. https://doi.org/10.1016/j.geoderma.2016.10.020

Šimůnek, J., van Genuchten, M.Th., Šejna, M., 2012. HYDRUS: Model Use, Calibration, and Validation. *Transactions of the ASABE* 55, 1263–1276. https://doi.org/10.13031/2013.42239

Smith J.U., Smith P., 2007. Environmental modelling. An introduction. Oxford University Press, Oxford

Spencer, J.W., 1971. Fourier series representation of the position of the sun. *Search* 2(5), p172

Tóth, B., Weynants, M., Nemes, A., Makó, A., Bilas, G., Tóth, G., 2015. New generation of hydraulic pedotransfer functions for Europe: New hydraulic pedotransfer functions for Europe. *European Journal of Soil Science* 66, 226–238. https://doi.org/10.1111/ejss.12192

United States Department of Agriculture USDA, 1951. Soil survey manual, U.S. Dept. Agriculture Handbook No. 18. Washington, DC

van Genuchten, M.Th., 1980. A closed-form equation for predicting the hydraulic conductivity of unsaturated soils. *Soil Sci. Soc. Am. J.* 44, 892–898.

Vanclooster, M., Viaene, P., Diels, J., Christiaens, K., 1996. *WAVE, A mathematical model for simulating water and agrochemicals in the soil and vadose environment*. Reference and user's manual (Release 2.1). Inst, for Land and Water Management, Katholieke Universiteit Leuven, Belgium.

Wolock, D., McCabe, G., 1999. Explaining spatial variability in mean annual runoff in the conterminous United States. *Climate Research* 11, 149–159. https://doi.org/10.3354/cr011149

Wösten, J.H.M., Lilly, A., Nemes, A. and Le Bas., C. 1998. Final Report on the EU funded project *Using existing soil data to derive hydraulic parameters for simulation models in* *environmental studies and in land use planning.* (CHRX-CT94-0639). DLO Winand Staring Centre. Report 156. Wageningen, The Netherlands.

Wösten, J.H., Lilly, A., Nemes, A., Le Bas, C., 1999. Development and use of a database of hydraulic properties of European soils. *Geoderma* 90, 169–185. https://doi.org/10.1016/S0016-7061(98)00132-3